


Mesenchymal Stem Cells of Different Origin-Seeded Bioceramic Construct in Regeneration of Bone Defect in Rabbit

Swapan Kumar Maiti¹  · M. U. Shivakumar¹ · Divya Mohan¹ · Naveen Kumar¹ · Karam Pal Singh²

Received: 5 April 2018 / Revised: 2 May 2018 / Accepted: 24 May 2018 / Published online: 10 July 2018

© The Korean Tissue Engineering and Regenerative Medicine Society and Springer Science+Business Media B.V., part of Springer Nature 2018

Abstract

BACKGROUND: Stem cell is currently playing a major role in the treatment of number of incurable diseases via transplantation therapy. The objective of this study was to determine the osteogenic potential of allogenic and xenogenic bone-derived MSC seeded on a hydroxyapatite (HA/TCP) bioceramic construct in critical size bone defect (CSD) in rabbits.

METHODS: A 15 mm long radial osteotomy was performed unilaterally in thirty-six rabbits divided equally in six groups. Bone defects were filled with bioscaffold seeded with autologous, allogenic, ovine, canine BMSCs and cell free bioscaffold block in groups A, B, C, D and E respectively. An empty defect served as the control group.

RESULTS: The radiological, histological and SEM observations depicted better and early signs of new bone formation and bridging bone/implant interfaces in the animals of group A followed by B. Both xenogenous MSC-HA/TCP construct also accelerated the healing of critical sized bone defect. There was no sign of any inflammatory reaction in the xenogenic composite scaffold group of animals confirmed their well acceptance by the host body.

CONCLUSION: *In vivo* experiments in rabbit CSD model confirmed that autogenous, allogenic and xenogenous BMSC seeded on bioscaffold promoted faster healing of critical size defects. Hence, we may suggest that BMSCs are suitable for bone formation in fracture healing and non-union.

Keywords Mesenchymal stem cells · Hydroxyapatite bioceramic · Allogenic · Xenogenic · Bone healing

1 Introduction

The process of fracture healing is unique, in which damaged bone restores its original architecture but it does not form a poorly organized replacement matrix, otherwise known as scar tissue, rather it regenerates the original

matrix and retains its mechanical properties. In order to repair bone defects, a combination of cells with osteogenic activity and appropriate scaffolding material can stimulate bone regeneration and its repair. A potential substitute for autologous transplantation should possess 3 elements: osteoprogenitor cells, osteoinductive factors, and an osteoconductive scaffold [1].

Stem cells from adult tissues are attractive materials for cell therapy and tissue engineering. These cells generally have restricted lineage potential when compared to embryonic stem cells, and this may be advantageous in certain therapeutic applications [2, 3]. Bone-marrow-derived mesenchymal stem cells (BMSCs) have proven to be beneficial in bone regeneration [4]. Bone marrow stem cells are pluripotent cells with the capability of

✉ Swapan Kumar Maiti
swapanivri@gmail.com; maiti_62@rediffmail.com

¹ Division of Surgery, ICAR-Indian Veterinary Research Institute (Deemed University), Izatnagar, Uttar-Pradesh 243122, India

² Centre for Animal Disease Research and Diagnosis, ICAR-Indian Veterinary Research Institute (Deemed University), Izatnagar, Uttar-Pradesh 243122, India

differentiating osteoblasts so that they have been used to facilitate bone repair [5]. Several studies have shown that seeding of cultured BMSCs on bioabsorbable implants can induce bone formation *in vivo* and lead to improved healing of critical-size bone defects [6].

Mesenchymal stem cells (MSCs) because of their self replication and osteogenic differentiation capabilities are regarded as an excellent source of cells for bone tissue engineering [7]. Autologous stem cells are not always preferable since the quality and quantity of such cells will be affected by metabolic diseases, old age, and osteoporosis [8]. Allogenic BMSCs might be preferable to xenogenic, but they are always not readily available. In addition, allogenic MSCs have the potential for carrying some diseases [9]. The use of non-autologous stem cells isolated from healthy donors offers a major advantage since these stem cells can be thoroughly tested and formulated into off-the-shelf medicine in advance [10]. Major attractive advantage of BMSCs as a source of cell transplantation is their low Immunogenicity. It is now well established that BMSCs are immune-privileged cells that do not elicit immune responses due to an absence of their immunologically relevant cell surface markers [11–13].

In the last two decades, many of the bone substitute materials have been evaluated to replace the necessity for autologous or allogenic bone. Among them, the feasibility of bioactive ceramics, bioactive glasses, biological or synthetic polymers, and their composites for bone tissue engineering has been studied [14–16]. Bioactive ceramics, namely calcium hydroxyapatite (HA), HA with tri-calcium phosphate (HA/TCP) and bioactive glasses, have been used as scaffold for bone reconstruction for many years [17–19]. They are termed ‘bioactive’ because they form an interfacial bond with tissues upon implantation and potentiate osteogenic activity as a result of surface modification when exposed to interstitial fluids. Bioceramic provides scaffold to support the attachment and migration of newly formed bone cells into the bone defect and also help in the formation of a capillary network through the newly formed bone. Bioceramic also acts as a carrier to deliver stem cells for osteogenesis and these bioactive inorganic materials are similar in composition to bone mineral that is of clinical importance.

Till now most of the xenogenic MSC transplantations for bone healing have been done from human to laboratory or large animal models of bone healing and between the two species of laboratory animals (rat and rabbit). The xenogenic transplantation of MSCs from small or large animal species to rabbit model of bone healing has not been attempted to the best of our knowledge. In this study, we investigated the potential of allogenic (rabbit) and xenogenic (sheep and dog) bone marrow-derived mesenchymal stem cells seeded on a biphasic bioceramic construct

(namely HA/TCP) to enhance osteogenesis in a critical size bone defect (CSD) in rabbit model.

2 Materials and methods

2.1 Experimental design

The male adult skeletally mature New Zealand white rabbits of 7 months to 1 year old and with a mean weight of 2.78 ± 0.36 kg were used in this study. They were maintained in separate cages, fed ad libitum and allowed to move freely during the whole period of study. For this purpose 36 animals were divided into six equal groups (each $n = 6$). These groups were treated and compared as follows: the radial 15-mm critical-size bone defect was filled with HA/TCP seeded with autogenous rBMSC (group A); HA/TCP seeded with allogenic rBMSC (group B); HA/TCP seeded with ovine BMSCs (group C); HA/TCP seeded with canine BMSCs (group D), cell free HA/TCP scaffold only (group E). In group F, the critical-size bone defect was left as such (untreated) and served as control.

Hematological parameters were evaluated preoperatively in order to rule out systemic diseases. Based on clinical examination and preoperative radiographs it was assessed that the experimental animals had no signs of bone or joint disease on the relevant limbs.

2.2 Bioceramic scaffold

A biphasic composite bioceramic comprising of calcium hydroxyapatite and tricalcium phosphate namely HA/TCP in the following percentage: calcium hydroxyapatite-65% and tricalcium phosphate 35%, and porosity of 200–450 μm was used as ceramic block. Each HA/TCP block was of 15 mm long and 5 mm in diameter were produced in an emulsion process [20].

2.3 Isolation and culture of rBMSC, oBMSC and cBMSC

Isolation, expansion and culture of rabbit BMSC (rBMSC), ovine BMSC (oBMSC) and canine BMSC (cBMSC) was performed as described earlier [21]. The BMSCs of different origin were used at 3rd passage in this study.

2.4 Seeding of BMSC into HP/TCP ceramic blocks

The third passage cells (six million) of rBMSC, oBMSC and cBMSC were resuspended in 4 ml of Dulbecco's modified Eagle Medium (DMEM) and were transferred into a 5 ml tube. The HA/TCP bioscaffold were incubated

at 4 °C in 50 $\mu\text{M ml}^{-1}$ fibronectin solution diluted in phosphate buffered saline (PBS) for 24 h. The HA/TCP blocks were then placed into the medium containing the cells. After continuous spinning for 1.5 h at 37 °C (35 rpm), the ceramic blocks were placed into a 6-well plate. The cell pellet obtained after centrifuging the media containing the cells at 800 g for 5 min was resuspended in 70 μl of culture medium and seeded on the ceramic blocks. This MSC seeded ceramic bioscaffold was then used in groups A, B C and D. In group E, only cell free HA/TCP bioscaffold was used at the defect site.

2.5 Surgical procedure

All the animals were provided 3 weeks time period for acclimatization to the environment prior to surgery. Animals were given general anaesthesia with xylazine hydrochloride (6 mg/kg, IM) and ketamine hydrochloride (60 mg/kg, IM). Under strict surgical asepsis, a medial approach to the radius bone was performed and a unilaterally critical-size bone defects were created in the radial diaphysis. A 3 cm medial incision was given over the radius, soft tissue was dissected and the radius was exposed by gentle separation of the surrounding muscles. To protect the ulna, a Hohmann retractor was placed in between ulna and radius. A 15 mm long osteoperiosteal critical-size bone defect was created with the help of an oscillating bone saw which was continuously irrigated with sterile cold saline to prevent thermal necrosis. The periosteum was removed from each side of the remaining radius. The bone defect was cleaned with sterile physiological saline and composite ceramic construct was placed into the bone defect as per treatment protocol for different groups. The stem cell- bioceramic construct was secured in position by suturing the bioceramic block in the bone defect with 2–0 absorbable sutures. The skin was sutured with non-absorbable nylon suture (Fig. 1). A custom designed wooden splint padded with sterile gauze was applied on the test bone for 1 week postoperatively.

2.6 Postoperative care

Regular dressing with antiseptic lotion was carried out for 5 days post surgery. Animals were administered ceftriaxone sodium (20 mg/kg) intramuscularly for 5 days. Meloxicam (0.15 mg/kg, IM) was given for the first 3 postoperative days as an analgesic agent. The animals were kept in an individual cages and allowed unrestricted weight bearing activity post surgery. The animals were sacrificed after 90 days of experiment.

2.7 Radiological assessment

Radiographs were taken using table top procedure at 14 mAs; 50 kVp and 90 cm FFD. Craniocaudal and mediolateral radiographs of each bone defect site were taken immediately after surgery to monitor the position of the implants. Subsequently radiographs were taken at 14, 30, 60 and 90 days postoperatively to record the acceptance or rejection of stem cell-bioceramic construct and the initiation and progression of bone formation and healing at critical size bone defect site. The radiographs were graded with slight modification of the scoring system reported earlier [22] (Table 1). Overall radiographic scores for each group were calculated by adding mean scores for each group at different time intervals. Resorption of bioceramic implant (HA/TCP) was qualitatively assessed.

2.8 Scanning electron microscopic assessment

The evaluation of new bone formation at defect site in different treatment groups was done by scanning electron microscopic (SEM) technique. The implants were explanted after euthanizing the animals on day 90 post surgery. Each specimen consisted of both fracture healing site and adjacent bone. The samples were fixed in 2% glutaraldehyde phosphate buffer solution for 24–48 h. After fixing in glutaraldehyde, two washings for 30 min each with

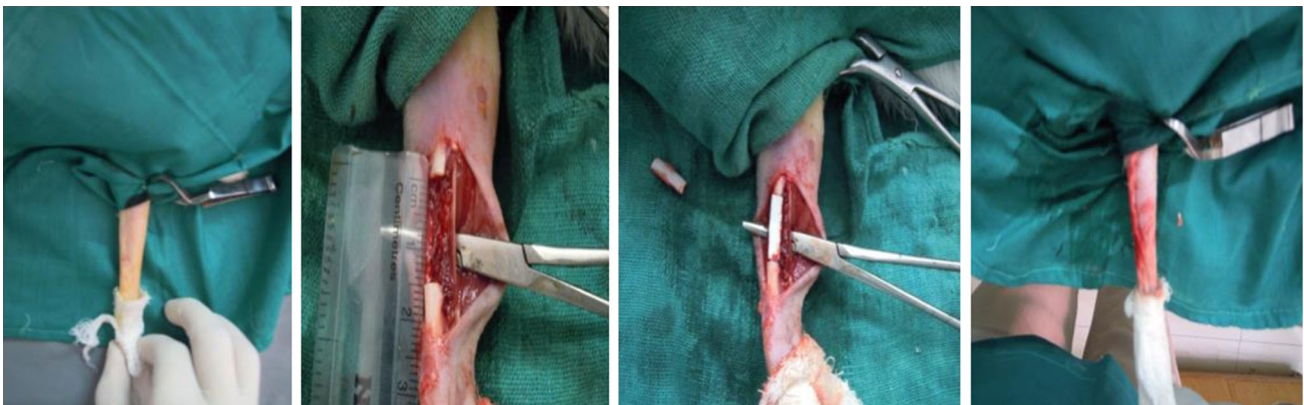


Fig. 1 Surgical procedures for creating 15 mm CSD of radius in rabbits

Table 1 Radiographic grading scale for degree of new bone formation and critical sized defect (CSD) healing

Description	Score
No change from immediate post-operative appearance	0
A slight increase in radio density distinguished from the implant	1
Recognizable increase in radio density of the implant with bridging of the cortex	2
Callus formation with complete defect bridging	3
Bridging at least one cortex with material of non-union radio density, easily incorporation of the implant suggested by obscurity of implant borders	4
Defect bridged on both proximal and distal sides with bone of uniform radio density, cut ends of the cortex still visible, implant and new bone not easy to differentiate	5
Same as grade 3, with at least one of four cortices obscured by new bone	6
Defect bridged by uniform new bone, cut ends of cortex no longer distinguishable, implant no longer visible	7
Complete union, complete new bone formation, complete cortex covered the defect, marrow cavity formed	8

phosphate buffer saline (pH 7.4) followed by distilled water was performed. Then the specimens were dehydrated in serial concentration of ethanol 30–100% for 30 min each. Thereafter, the specimens were dried with Hexamethyldisilazine (HMDS) for 20 min. Specimens were mounted on aluminum stubs using adhesive silicon tape. After the golden ion sputtering done on Jeol ion sputter Model JFC 1600 at 7–10 mA and 1–2 kv for 15 min. Finally, the specimens were observed under scanning electron microscope (Jeol JSM 6610 LV, Japan) at appropriate acceleration voltage and magnification range of the unit calibrated for the study of their different surfaces to identify the orientation and distribution of newly formed osseous tissue and distribution or absorption of construct at the bone defect site.

2.9 Histopathological assessment

The test bones were collected from the animals sacrificed on day 90 postoperatively and a 2.5 cm long piece of radius including the site of the defect and normal host bone on both sides was cut using hexa saw. The bone segments were washed thoroughly with normal saline and fixed in 10% formalin for 48–72 h. The bone sections were decalcified in Goodling and Stewart's solution containing 15 ml formic acid, 5 ml formalin and 80 ml distilled water. The sections were checked regularly for the status of decalcification. The completion of decalcification was assessed by flexibility, transparency and pin penetrability of the bone sections. The tissues were processed in a routine manner and 4 μ thick longitudinal and transverse sections were cut and stained with Hematoxylin and Eosin (H&E) as per standard procedure. The stained sections were examined under different magnification in a light microscope for cellular reaction, healing process and fate of the implanted bioceramic. Bone healing was assessed in each group

according to modified Kaveh et al. [22]. Histopathological scoring system was presented in Table 2.

Radiographic, histological and scanning electron microscopic examinations in this study were performed blindly.

2.10 Statistical analysis

Data analysis was performed by using general linear model (GLM) to identify the effect of various fixed factors on the dependent variable using SPSS software package (version 16). Mean values and standard deviations were calculated. The nonparametric data were analyzed with Kruskal–Wallis test. Values of $p < 0.05$ were considered significant.

3 Results

3.1 Clinical assessment

In all experimental groups A, B, C, D, E except the control group F, the food and water intake returned to normal on day 3 while in the later on day 7. Weight bearing was mild to moderate on the operated limb from day 2 post surgery in all groups except group F. Complete weight bearing was seen on day 7 after surgery in all animals of groups A, B, C, D and E after removal of wooden splint. Whereas, in control group F the animal did not bear weight normally throughout the study period. The implanted biomaterials (HA/TCP) did not shown any signs of inflammation, irritation or infection. The skin wound healed uneventfully.

3.2 Radiographic assessment

Due to overlapping of the radius by adjacent ulna bone in craniocaudal view, the radiographic evaluation of the defect site at different intervals mostly involved analysis of

Table 2 Histological grading scale for degree of healing

Scale	Description	Score
Quality of union	No sign of fibrous or other union	0
	Fibrous union	1
	Fibro cartilage or cartilage union	2
	Mineralized cartilage and immature bone union	3
Bone union		4

Table 3 Radiographic score (mean \pm SD) of different groups at different time intervals

Groups	Day 0	Day 14	Day 30	Day 60	Day 90	Total
Group A	0 \pm 0.00	1.2 \pm 0.09*	2.5 \pm 0.34	3.8 \pm 0.43*	4.5 \pm 0.45*	12.00 \pm 0.32**a
Group B	0 \pm 0.00	0.9 \pm 0.45	2.9 \pm 0.22*	3.4 \pm 0.23*	4.02 \pm 0.05*	11.22 \pm 0.23**b
Group C	0 \pm 0.00	0.6 \pm 0.78	2.7 \pm 0.67	2.9 \pm 0.57	3.98 \pm 0.78*	10.18 \pm 0.70**c
Group D	0 \pm 0.00	0.7 \pm 0.87	2.9 \pm 0.56*	3.5 \pm 0.23*	4.1 \pm 0.77*	11.20 \pm 0.60**c
Group E	0 \pm 0.00	0.3 \pm 0.12	1.45 \pm 0.66	2.1 \pm 0.45	2.2 \pm 0.12	06.05 \pm 0.33**de
Group F	0 \pm 0.00	0 \pm 0.00	0.2 \pm 0.22	0.3 \pm 0.12	0.44 \pm 0.89	00.94 \pm 0.24 ^d

Different superscripts indicates mean value differs significantly at $p < 0.05$ between groups

**Mean value differ significantly at $p < 0.01$ within the group

*Mean value differ significantly at $p < 0.01$ within the group

mediolateral views of the radiographs. Radiographic scores (mean \pm SD) in all six groups at different time intervals are presented in Table 3. Mediolateral views of radiograph of animals of six groups are presented in Fig. 2A–F.

The critical size defect was clearly visible with cut edges of the bone almost at the center of the radial diaphysis in all the animals of control group at day 0 and this area was filled by tissue engineered bioceramic block in other test groups that looked relatively denser than the adjacent bone.

In group A, at day 14, there was no evidence of callus formation but there was increase in radiodensity of the construct with little periosteal reaction at the cut edges of the host bone. It was observed that there was mild resorption of the construct which started at day 30 and at the end of day 60 the resorption was moderate. There was close attachment of the autogenous construct with the adjacent ulna and bridging between construct and cut end of the host bone at day 60. Whereas, excellent new bone formation was noticed and bridging of construct with host bone and adjacent ulna was complete at day 90.

In group B, bridging of the bone and construct at cut ends was seen from day 30 onwards. At day 60, there was complete bridging of composite allogenic construct with the host bone at all the surface of contact along with adjacent ulna which indicating the formation of new bone. At day 90, excellent new bone formation, which was evident radiographically by resorption of bioceramic block and bridging of construct completely with the host bone, and bioceramic block, had lost its shape completely.

The bridging between host bone and xenogenic construct in both proximal and distal interfaces was evident at

day 30 in groups C and D. At day 60, there was close union between composite scaffold and the host bone as well as with adjacent ulna. A major portion of the construct underwent resorption and the boundary between construct and host bone disappeared which indicating the construct had been mostly replaced by new bone at the end of 90 days. In groups C and D there was complete bridging on both proximal and distal ends with host bone of uniform radiodensity, which indicating deposition of new osteoid bone into the bioceramic construct by the osteoprogenitor cells. The bone formation was more or less similar in both C and D groups, however, bone formation in group D was better than group C. In animals of groups C and D there was no graft rejection process, which was radiographically evident by absence of inflammatory response in and around the critical size defect area. At this stage both the xenogenic transplanted groups, showed better bone formation compared to control and ceramic group, but there was less bone formation in comparison to autologous and allogenic group.

In group E, there was gap between the bioscaffold and the cut ends of the host bone till day 90. There was no evidence of bridging at either proximal or distal end of the ceramic scaffold with the host bone. New bone formation was very negligible. In control group, at day 30, there was fibrous dense tissue appearance near the defect margins. The defect was clearly visible without any callus formation. At day 90, more fibrous tissue at the cut ends of radius, but there was no union of the ends by any of the structure.

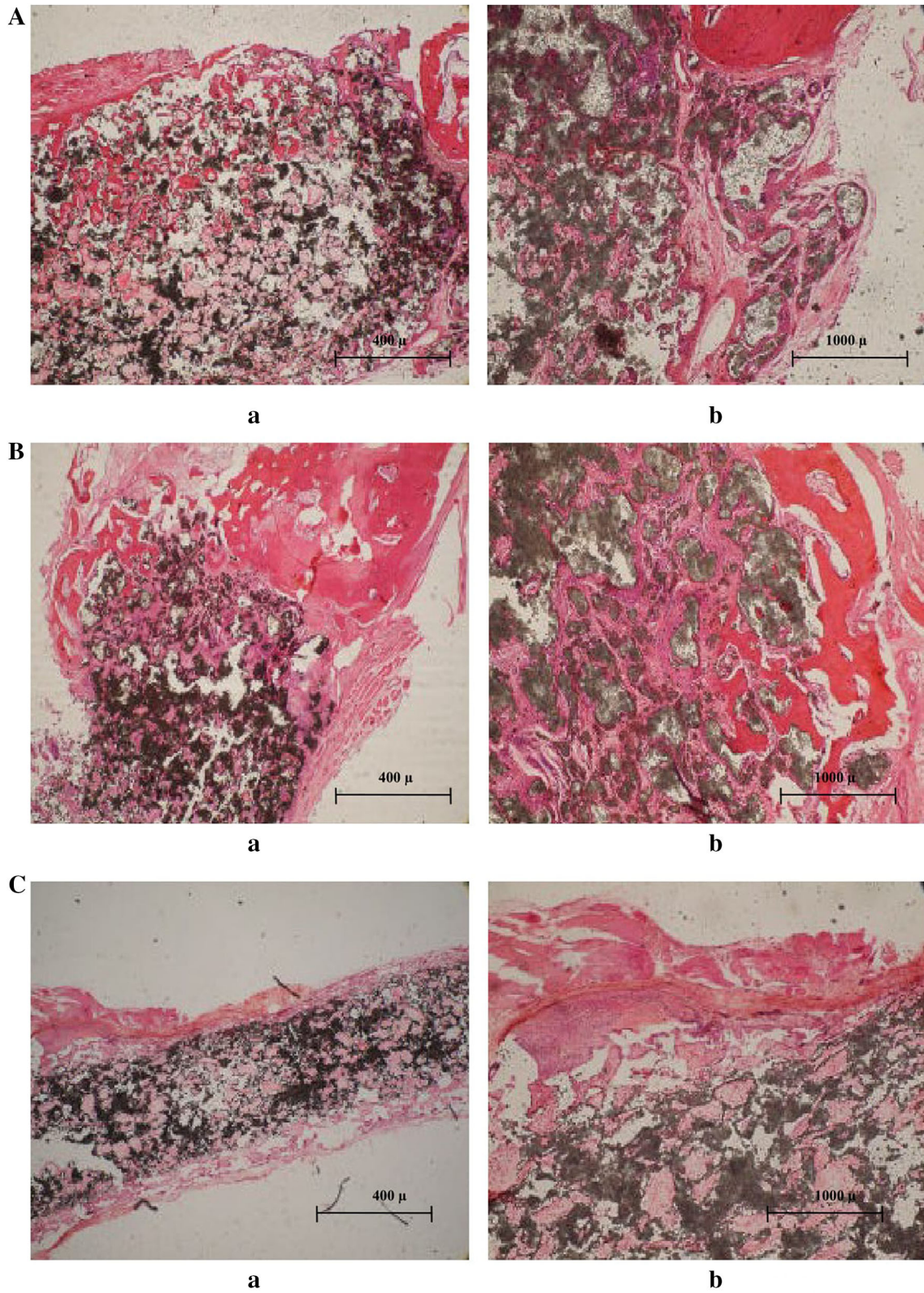
The total radiographic score for healing of critical size defect in different groups over a period of 90 days was

Fig. 2 Sequential mediolateral radiographs of group A (**A**); group B (**B**); group C (**C**); group D (**D**); group E (**E**); and group F (**F**) at different time intervals



Fig. 2 continued





◀ **Fig. 3** Histopathological section at bone defect site of different groups at day 90; **A(a)** longitudinal section of gr A showed mature and immature bony trabeculae with residual implant and formation of normal periosteum, H&E, $\times 40$; **A(b)** transverse section of gr A showed osteoprogenitor cells at defect site, H&E, $\times 100$; **B(a)** longitudinal section of gr B showed formation of periosteum, new bone at the junction of host bone and implant, H&E, $\times 40$; **B(b)** transverse section of gr B showed mature bone and osteoprogenitor cells in bone formation, H&E, $\times 100$; **C(a)** longitudinal section of gr C showed the junction of host bone and implant covered with normal periosteum, formation of mature and immature bony trabeculae and absence of any inflammatory cells, H&E, $\times 40$; **C(b)** longitudinal section of gr C showed the mature bone and osteoprogenitor cells in bone formation at the defect site, H&E, $\times 100$; **D(a)** longitudinal section of gr D showed host bone and implant covered with normal periosteum. Mature bone was more at the junction and immature bony trabeculae with residual implant at the periphery, H&E, $\times 40$; **D(b)** transverse section of gr D showed the mature bone and osteoprogenitor cells in bone formation with absence of inflammatory cells, H&E, $\times 100$; **E(a)** longitudinal section of gr E showed host bone and implant with less periosteum surrounding the implant. Only immature bony trabeculae with residual implant were visible, H&E, $\times 40$; **E(b)** transverse section showed only little mature bone without osteoprogenitor cells and inflammatory cells, H&E, $\times 100$; **F(a)** longitudinal section of gr F showed the fibrous tissue proliferation at the cut ends without any bone formation, H&E, $\times 100$; **F(b)** longitudinal section of gr F showed only fibrous connective tissue with complete absence of osteoprogenitor cells. H&E, $\times 200$

significantly higher in group A followed by groups B, D, C, E and F (Table 3).

3.3 Histopathological assessment

The histopathological observations at different time intervals in various groups are presented in Fig. 3A–F. In group A, the periosteum formation was normal and completely surrounded the scaffold. Defect was completely filled with bony trabeculae which was mature at the junction and immature at the centre of the defect. Most of the constructs were substituted by newly formed bone with residual scaffold material that was visible at the defect site. The stained tissue section showed varying colors of pink with

mineralized matrix seen as bright pink and the cell nuclei stained dark purple. At higher magnification, osteoblastic lineage was clearly observed around the new bone with many osteocytes (Fig. 3A).

In group B, newly formed bone was observed in all the animals at defect sites and the bioceramic scaffold was completely surrounded by periosteum. The trabecular bone was observed throughout the tissue engineered construct, which was more mature at the junction of the defect compared to centre of the bone defect (Fig. 3B). Most of the scaffold was substituted by new bone with minimal residual ceramic material. At the junction of the defect site, there was higher amount of mature bone formation (Fig. 3B). The gap between the trabecular bones was minimal. Lamellar bone formation was seen into porous scaffold at higher magnification.

In groups C and D, the tissue engineered construct/bioscaffold was surrounded by the normal periosteum in all the animals (Fig. 3C, D). The new bony trabeculae were observed throughout the bioceramic construct. In higher magnification at the junction of the construct, the lamellar bone formation was seen along with proliferating osteoprogenitor cells. The residual material was minimal indicating resorption of ceramic material in these groups. The new bone stained light pink and ceramic material had a shadowy white appearance, loose connective tissue stained light pink and cells stained dark purple (Fig. 3C, D). There were no signs of inflammatory reaction around the construct in any of the animals of the groups C and D.

In group E, the periosteal reaction surrounding the scaffold was minimal and formation of trabecular bone was very less (Fig. 3E). Most of the scaffold was filled with fibrous connective tissue which stained light pink colour throughout the scaffold (Fig. 3E). No phagocytes were observed in the evaluated sections indicating high biocompatibility of HA/TCP ceramic. In group F, there was no evidence of bone formation in any of the animals at the defect site (Fig. 3F). There was proliferation of dense fibrovascular connective tissue and inflammatory reaction at the junction of the defect (Fig. 3F). The entire gap was filled with fibrovascular tissue.

The total histological scores of bone healing for different groups are presented in Table 4. Group A had the highest scores, followed by groups B, D, C, E and F.

Table 4 Histological score of different groups at 90th day

Implanted group	Histological score Average \pm standard deviation
Group A	3.0 \pm 0.23 ^a
Group B	2.7 \pm 0.65 ^b
Group C	1.9 \pm 0.63 ^c
Group D	2.2 \pm 0.32 ^c
Group E	0.75 \pm 0.23 ^d
Group F	0.2 \pm 0.01 ^d

Different superscripts indicates mean value differs significantly at $p < 0.05$ between groups

3.4 Scanning electron microscopic (SEM) observations

The scanning electron microscopic observations are presented in Fig. 4A–F. A close contact without intervening soft tissue was seen between the bones and construct in the group A. The osseous tissue was predominantly seen at the junction of construct and host bone. There was presence of

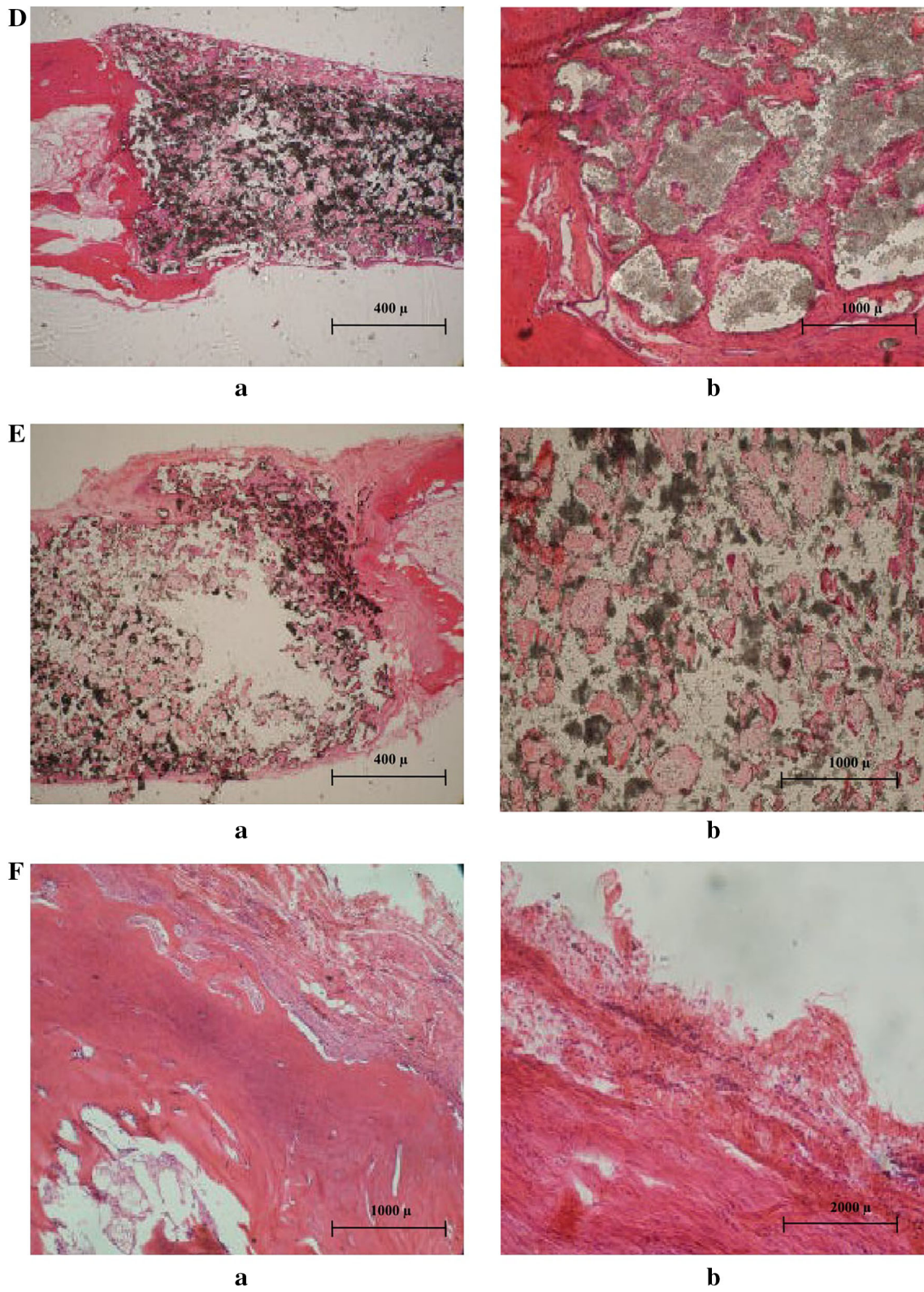


Fig. 3 continued

bony tissues inside macropores of ceramic construct throughout surface of the block. The micron-sized micropores inside the block were infiltrated by bony tissue and the collagen fibrils demonstrated a direct bone-to-material contact (Fig. 4A). In group B, there was strong bridging of construct with the host bone by mature osseous bony structure. The bone formation was seen throughout the surface of ceramic-cell construct inside the micropores (Fig. 4B). Collagen fibrils were arranged in irregular manner and their density was more. In groups C and D, bioceramic construct was in close contact with the host bone by newly formed osseous tissue. The entire macropores of the bioceramic construct was filled with woven bone. The resorption of hydroxyapatite, growth of new bone from inside to outside in the macropores of ceramic construct along with formation of collagen fibers was also evident (Fig. 4C, D). In group E, bridging of bioceramic construct with host bone was not so strong unlike other test groups. The surface of the bioceramic block revealed more of the implant material as such, which was indicating less resorption of ceramic material (Fig. 4E). Inside the macropores, new bone formation was scanty. In group F, there was no bone formation at the entire length of the defect. The defect was filled with fibrous tissues (Fig. 4F).

4 Discussion

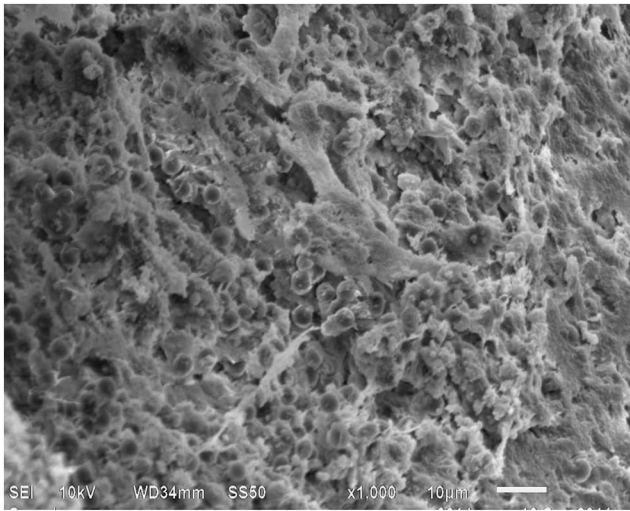
The present study was conducted to evaluate the potential of cultured autogenic, allogenic and xenogenic bone marrow derived mesenchymal stem cells (BMSC) seeded on a resorbable bioceramic scaffold (HA/TCP) in the regeneration of bone at critical-size-defect in rabbit model.

The critical-sized defect in rabbits creates a weight bearing model in which the implanted bioscaffold sensitizes the adjacent mechanical load and structural rapport to the bone defect [4, 16]. The ulna itself serves as an internal splint for the radius, so no external fixation is needed. In spite of this, we have used a custom-designed external splint in this study which was maintained for 7 days post bone defect. Human mesenchymal stem cells transplantation for bone regeneration in a rabbit critical-size defect (15 mm) has been reported [4], but the regeneration potential of allogeneous and xenogeneous mesenchymal stem cells are till now not reported. Hence, we created critical-sized radial diaphyseal defect in rabbits and transplanted autogenous, allogeneous along with two types of xenogeneous BMSC and found that this model was very much suitable for this experiment.

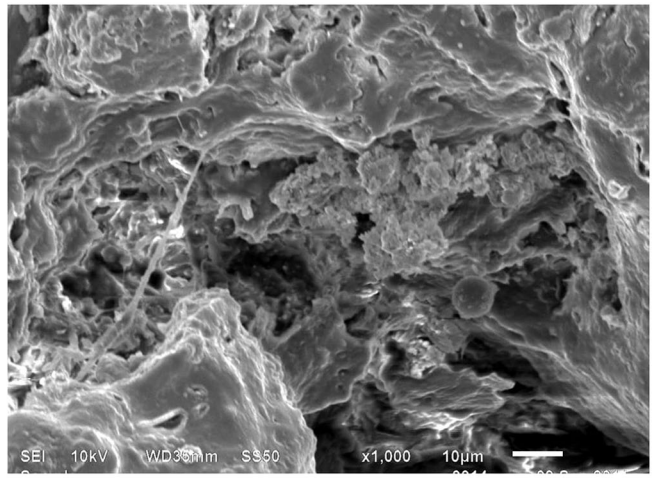
Healing of segmental bone defects and massive bone defects constitute a major challenge to orthopedic and

trauma surgery. A bone defect may not heal because of local factors like infection, mechanical instability, inadequate vascularity, poor bone contact, magnitude of injury and systemic conditions like malnutrition, diabetes, and metabolic bone disorders [23]. When the normal endogenous mechanisms are not able to restore the lost bone, such as in non-union fractures, removal of benign bone tumors, or large-scale traumatic bone injury, surgical intervention is necessary. The fracture model (CSD) selected for the present investigation was thus need based and the outcome would hold potential for clinical application in animals and humans of large segmental defect.

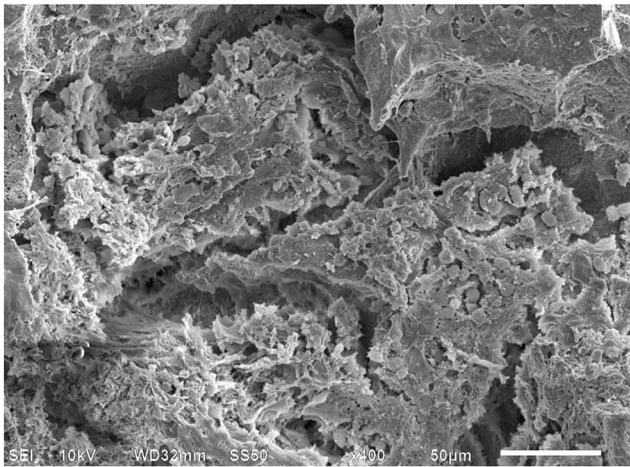
No significant new bone formation and bridging the bone defect were found in any animal in the control group in which the bone defect was left untreated. On day 90, there was fibrous dense tissue appearance near the defect margins along with small quantity of bone regeneration, which was limited to the margins of defects. In this study main aim was to investigate the potentiality of autogenic, allogenic and xenogenic BMSC in bone healing in critical-size defect; empty bioscaffold were used as an additional control group. The scaffold used in the present study was HA/TCP—a biphasic bioceramic. In the bioceramic group (E), osteogenesis was minimal and there was no evidence of bone healing at either proximal or distal end of ceramic block with the host bone at day 90 post bone defect. The bioceramic (HA/TCP) alone is not able to lead to healing of critical-size-defects. Although, more new bone formation could be seen in animal treated with HA/TCP alone compared to empty controls, but failed to bridge the defect at day 90 post defect. Similarly, reconstruction of 15 mm segmental bone defect in the rabbit ulna using porous poly(lactic-co-glycolic acid) (PLGA) scaffold failed to bridge completely even at 12 weeks post implantation [24]. In this study we observed, if this bioceramic implant HA/TCP even kept for further long duration, it might not be able to bridge the critical-sized defect completely. The type and form of biomaterial, the pore size and pore distribution, interconnectivity and the resorption of the biomaterial can influence the *in vivo* bone formation was reported [25]. In this study the biomaterial used were manufactured in blocks which cannot be compared to other studies where granules or powders were used [4]. For example, more new bone formation was evidenced with the use of HA/TCP powder than HA/TCP blocks [26]. The HA/TCP blocks were used as scaffold in this study owing to their better biomechanics and the easier future clinical use in segmental bone defects [27]. The biomaterial used in the present study comprised open pores in the range of 200–450 μm , and geometry wise; it is fully interconnected with a large surface area to volume ration and composed of 65% calcium hydroxyapatite and 35% tricalcium phosphate. This property seems to have improved the migration and



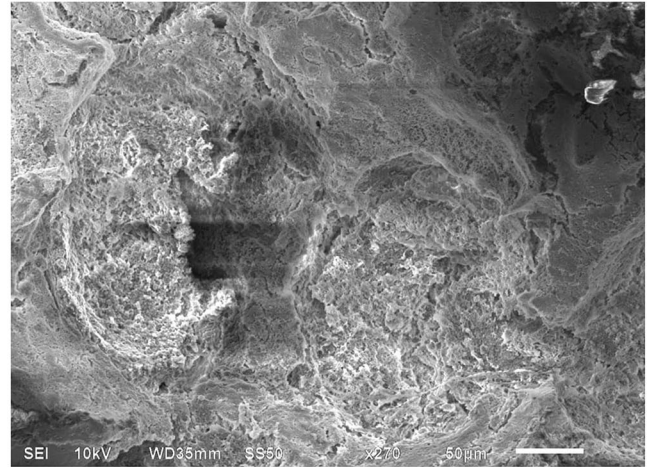
A



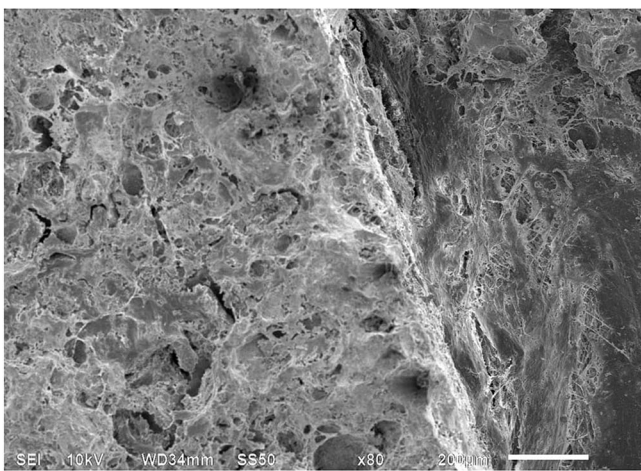
B



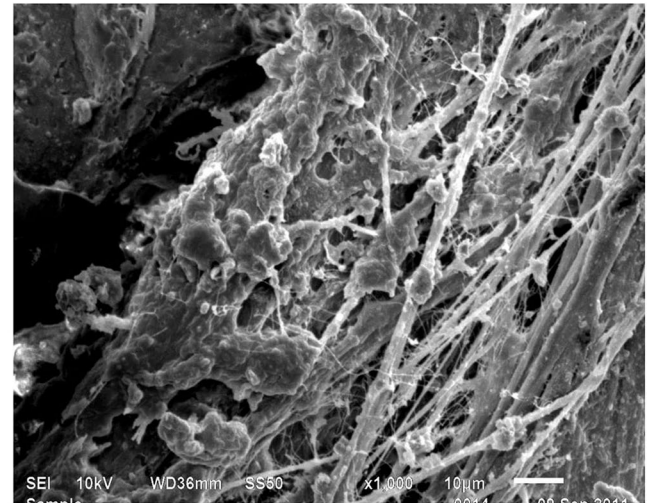
C



D



E



F

◀ **Fig. 4** SEM photomicrograph of undecalcified bone sections of different groups at day 90; **A** sections of gr A showed compact granular bone, $\times 1000$; **B** sections of gr B showed the granular bone within the micropores of HA/TCP blocks, $\times 1000$; **C** sections of gr C depicted the ingrowths of bone from inside to outside in the macropores of HA/TCP blocks, the collagen fibers were also visible, $\times 400$; **D** sections of gr D revealed deposition of compact bone inside macropores of HA/TCP block, $\times 270$; **E** sections of gr E showed some empty macropores in the HA/TCP block, $\times 100$; **F** sections of gr F depicted the bundle of fibers connective at the defect site, $\times 100$

distribution of osteoprogenitor cells throughout the scaffold material. The HA/TCP blocks caused close union between scaffold and adjacent ulna in some animals due to its osteoconductive properties, which seems to be beneficial in not only uniting the adjacent splint bone near the defect site, but also it provided further mechanical stability to the injured bone [16].

Autogenous BMSC seeded on HA/TCP bio-scaffold was transplanted in critical-size-defect in group A and revealed extensive new bone formation compared to HA-TCP alone. Radiological, histological and SEM analysis showed bony union between the scaffold and cut ends of the host bone as well as with the adjacent ulna. This observation confirms previous *in vivo* and *in vitro* experiments which demonstrated the benefit of the addition of mesenchymal stem cells on bioscaffold for improved osteogenesis [4, 16]. Mesenchymal stem cells are non-hematopoietic stromal stem cells that are capable of self-replication and differentiating. These cells contribute in the regeneration of mesenchymal tissues such as bone, cartilage, ligament, tendon, muscle, and adipose tissue. MSCs promote infiltration of osteoprogenitor cells, and thus enhance their subsequent mineralization and bone formation [24, 28]. The osteogenic potential of MSCs has been well defined, as evidenced by bone formation following transplantation of MSCs *in vivo* and *in vitro* [29]. Recent studies with coupling MSCs to porous scaffolds have been successful for bone tissue engineering [30, 31]. MSC-derived osteoblasts cells are anchorage dependent and require a matrix in order to survive and flourish. So the selection of a suitable scaffold is another important criterion to be considered to fabricate a tissue-engineered construct. Inert, bio-active ceramics have an excellent biocompatibility and outstanding biological property, which encourage their use in bone reconstructive surgery [18]. Bioactive ceramics, namely HA, HA/TCP have been used as scaffold for bone reconstruction for many years [17]. Synthetic materials such as calcium phosphate bioceramics play an important role in bone reconstruction because of their unlimited availability, excellent biocompatibility, osteoconductivity and even more recently osteoinductivity [32]. Daculsi [6] demonstrated the efficiency of calcium phosphate

bioceramics in human as well in canine for bone reconstruction. The effect of cultured autologous MSCs loaded in porous HA/TCP ceramic cylinders on the healing of critical sized segmental defects in dogs has been evaluated and concluded that it can be used as an alternative to autogenous bone graft in critical-sized-defects of long bones [7]. Similar results also have been observed by using HA in sheep long bone defect model [33]. MSCs loaded with 56:44 and 20:80 HA/TCP demonstrated the greatest amount of bone formation with least amount in 100% TCP and 100% HA in canines [9]. In this study, the autologous MSC transplanted group of animals showed excellent bone formation, which was evident radiographically, histologically and SEM analysis by resorption of bioceramic block and bridging of block completely with the host bone, which had lost its shape completely. This increased osteogenesis could be due to conversion of mesenchymal stem cells into osteoblasts [34].

In this study, allogenic BMSC seeded on HA/TCP bio-scaffold was transplanted in critical-size-defect in group B and also showed abundant new bone formation, that was evident radiographically, histologically and SEM analysis by bridging of bioceramic block completely with the host bone at all surface of contact by the newly formed osseous structure. Similar observations of new bone formation using allogenic BMSC seeded in bioceramic scaffold were reported at 12 weeks in rabbit CSD model [4, 22, 35, 36]. Bruder [37] and Arinze [9] also reported new bone formation and bridging the defect in dogs using autogenic and allogenic mesenchymal stem cells. MSC are regarded as an excellent source of cells for bone tissue engineering because of their self replication and osteogenic differentiation capabilities [7]. Studies using MSCs for bone regeneration have demonstrated that seeding MSCs could not only provide an osteogenic cell source for new bone formation, but also secrete growth factors to recruit native cells to migrate to the defect site [38]. The use of autologous stem cells is not always desirable since the quality/or quantity of such cells will be affected by old age, osteoporosis, and metabolic diseases [8]. Stem cell function may also be pathologically impaired as demonstrated in diabetes and heart disease [39]. Certain disease-causing genotypes may preclude therapeutic use of autologous stem cells due to the inherent genetic defects [40, 41].

Significant new bone formation and close bony union of scaffold with the host bone at both cut ends as well as adjacent ulna was seen in groups C and D, where xenogenic-ovine and xenogenic-canine BMSC seeded bioscaffold (HA/TCP) were transplanted respectively in critical-size defect in rabbits. In both groups, radiological, SEM and histological analysis confirmed new bone formation bridging both the proximal and distal cut ends with host bone of uniform radio density, which indicates deposition

of new osteoid tissue into the bioceramic block by the osteoprogenitor cells. Histopathological analysis and SEM study showed newly formed bony tissue within the implantation site, well-differentiated mineralized lamellar bone surrounding the HA/TCP granules and the presence of osteoid border at the surface of new bony trabeculae after 90 days postsurgery. Direct ossification of the scaffold and dense lamellar bone were also noticed in some animals of these groups, suggest the possibility of direct formation of osteoblasts from the osteoprogenitor cells by the osteogenic and osteointegration effect of mesenchymal stem cells. There were no signs of any inflammatory reaction to the composite scaffold in any of the animals of groups C, D which confirmed that these composite constructs were well accepted by the host body. No phagocytes were observed in the evaluated histological sections, which indicated HA/TCP ceramics were highly biocompatible. Niemeyer [42] reported new bone regeneration by 8 weeks after xenogenic transplantation of human mesenchymal stem cells in a critical size bone defect in sheep. Similar observations also reported by Jager [43] in critical size femoral defect after xenotransplantation of cord blood-derived stem cells seeded onto a collagen/TCP bioscaffold. Both the xenogenic transplanted groups C and D showed better bone formation in comparison to control group F and bioceramic group E, but less bone formation compare to autogenic group A and allogenic group B. In xenogenic group of animals, the histological feature revealed normal periosteum surrounding the scaffold. The formation of new bone was seen in both groups C and D, but the extent of mature trabeculae bone was more in group D animals compared to group C. Scanning electron microscopic studies revealed that the bone formation was seen throughout the surface of the composite scaffold inside the micro pores. Collagen fibrils were arranged in irregular fashion and their density was higher in group D compared to group C. Kim [5] also showed that xenogenic BMSC loaded onto compression resistant matrix (CRM) survived and generate new bone when placed into the lumber spine of rabbits without immunosuppression. Human MSC also had ability to repair of vertebral injuries in porcine model [44].

In the ongoing search for a reliable source of stem cells for tissue regeneration, research in the field of xenotransplantation (cross species transplantation) has grown tremendously in last few years. Overcoming the immunologic hurdle of cross species transplantation as well as the problem of cross-species pathogen infectivity, i.e. xenozoonosis, are the scientific challenges facing the field. Among the cell sources explored for cell therapy, mesenchymal stem cells (MSCs) have captured growing interest for cell transplantation because of their low immunogenicity. Recently, several studies have reported that BMSC may be immune-privileged cells that do not

elicit immune response due to an absence of their immunologically relevant cell surface markers. BMSCs are also known to inhibit proliferation of T lymphocytes, B lymphocytes, dendritic cells, and natural killer cells [45–47]. The immune phenotype of culture-expanded MSCs is widely described as MHC Class I+, MHC Class II+, CD40-, CD80-, and CD86-, which is regarded as non-immunogenic, suggesting that MSCs may even trespass species defense barriers [11–13]. These attributes have prompted the use of MSC in allogenic and xenogenic transplantation for tissue regeneration.

In control, *in vivo* study revealed that no sign of osteogenesis or bone healing was observed in a radial segmental defect of 15 mm. While there was little sign of osteogenesis in scaffold group; however, it provided very good mechanical as well as structural support to the defect, but it was unable to bridge the bone defect at day 90 post implantation. It was observed that, osteogenesis was better in HA/TCP scaffold-MSC seeded groups than the group where only scaffold was applied, probably due to the addition of MSCs, which promote infiltration of osteoprogenitor cells, and thus enhance their subsequent mineralization and bone formation. Among the MSC transplantation groups, osteogenesis was better in autogenous group followed by allogeneous and xenogeneous groups. Both xenogeneous MSCs seeded bioceramic construct accelerated the healing of critical sized bone defect. Among the two xenogeneous groups, canine MSC seeded bioceramic construct stimulated the formation of abundant bony tissue bridging both proximal and distal interfaces as well as with adjacent ulna. Ovine MSC-seeded construct also accelerated new bone formation and bridging the defect but osteogenesis was comparatively less when compared to canine-MSC transplanted group. The HA/TCP biphasic bioceramic was acted as suitable bioscaffold for development of MSC-seeded tissue engineering construct for bone regeneration because of their biocompatibility and osteoinductivity.

Bone healing is a complex process where damaged bone restores its original architecture through a cascade of molecular and cellular events [48]. There is growing interest in the application of different types of mesenchymal stem cells (MSCs) in order to significantly improve bone repair and regeneration due to their self-replication, osteogenic differentiation capabilities and immunomodulatory effects. MSCs have been implanted in association with different bioscaffolds to rebuild bone. Different experimental and pre-clinical studies have proved that MSCs can accelerate bone healing and bone regeneration, however, the exact molecular mechanism of MSCs towards bone healing has not fully elucidated but different scientists revealed that different growth and trophic factors or cytokines released from MSCs which are responsible for

their osteogenic activity. Two families of growth factors appear to stimulate osteoblast differentiation from MSCs: the Wnt (a portmanteau of Wingless and integration I family) and the bone morphogenetic proteins (BMPs). Wnt proteins are a family of 19 highly conserved secreted glycoproteins that play essential role during bone development and tissue homeostasis. The importance of the canonical Wnt signaling in bone is well acknowledged. It is established that Wnt/ β -catenin activity is essential for bone development. BMPs are growth factors which belong to the transforming growth factor beta (TGF- β) superfamily. Among 20 BMP members, BMP-2, BMP-7 are very important growth factors associated with bone regeneration and bone healing. Similarly Runx 2 belongs to Runx family is also associated with bone healing [49]. In addition, various paracrine factors released by mesenchymal stem cells which play an important role in bone regeneration. The secretion factors include endothelial growth factor (EGF), fibroblast growth factor (FGF), vascular endothelial growth factor (VEGF), insulin-like growth factor (IGF), transforming growth factor (TGF) etc. are released from the MSCs during their osteogenic differentiation process induce recruitment and differentiation of osteogenic progenitors. The beneficial effects of MSCs include immunomodulatory effects, stimulation of angiogenesis, anti-apoptotic effects in osteoblastic lineage cells, recruitment of host MSCs/progenitor cells, and stimulation of their differentiation into osteoblasts [50]. Better osteogenesis found in autologous cell transplantation than other groups may be due to their less immunogenicity and better cell adaptability.

Large bone defects resulting from extensive trauma, non-union, delayed union or tumour resections are common clinical problems. Despite the usefulness that minimally invasive surgery and osteosynthesis have brought fracture management and bone healing, there are still many occasions where bone healing remains challenging. In these cases uses of mesenchymal stem cells from different origin may proved helpful and could promote bone regeneration in a large bone defect as in this study we observed uses of mesenchymal stem cells from different origin accelerated bone healing. However, further experiment and clinical trail are needed for examining the beneficial effect of mesenchymal stem cells of different origin-seeded on biomaterials in large bone defects in clinical cases.

Acknowledgement The authors wish to thank Prof. H. Varma, Sree Chitra Tirunal Institute for Medical Sciences and Technology, Trivandrum, Kerala (India) for his technical assistance for designing and preparation of HA/TCP bioceramic.

Author contributions SKM conceived and designed the study. SKM and SMU performed the experiments. KPS performed the histological

analysis. SKM, SMU, KPS and NK analyzed and interpreted the data. SKM, SMU, and NK contributed to research infrastructure. SKM and DM wrote the paper. All authors have given approval to the final version of the manuscript.

Compliance with ethical standards

Conflict of interest The authors declare that they have no conflict of interest.

Ethical statement This study was conducted after getting approval from the ICAR-IVRI—Institute Animal Ethics Committee for Animal Care and Animal Experimentation [IAEC, No-F. 1-53/2012-13-JD (Research)].

References

- Lane JM, Tomin E, Bostrom MP. Biosynthetic bone grafting. *Clin Orthop Relat Res.* 1999;367:S107–17.
- Barry FP, Murphy JM. Mesenchymal stem cells: clinical applications and biological characterization. *Int J Biochem Cell Biol.* 2004;36:568–84.
- Barrilleaux B, Phinney DG, Prockop DJ, O'Connor KC. Review: ex vivo engineering of living tissues with adult stem cells. *Tissue Eng.* 2006;12:3007–19.
- Niemeyer P, Szalay K, Luginbühl R, Südkamp NP, Kasten P. Transplantation of human mesenchymal stem cells in a non-autogenous setting for bone regeneration in a rabbit critical-size defect model. *Acta Biomater.* 2010;6:900–8.
- Kim HJ, Park JB, Lee JK, Park EY, Park EA, Riew KD, et al. Transplanted xenogenic bone marrow stem cells survive and generate new bone formation in the posterolateral lumbar spine of non-immunosuppressed rabbits. *Eur Spine J.* 2008;17:1515–21.
- Daculsi G, Passuti N, Martin S, Deudon C, Legeros RZ, Rahe S. Macroporous calcium phosphate ceramic for long bone surgery in human and dogs. Clinical and histological study. *J Biomed Mater Res.* 1990;24:379–96.
- Bruder SP, Kraus KH, Goldberg VM, Kadiyala S. The effect of implants loaded with autologous mesenchymal stem cells on the healing of canine segmental bone defects. *J Bone Joint Surg Am.* 1998;80:985–96.
- Ettinger MP. Aging bone and osteoporosis: strategies for preventing fractures in the elderly. *Arch Intern Med.* 2003;163:2237–46.
- Arinzech TL, Peter SJ, Archambault MP, van den Bos C, Gordon S, Kraus K, et al. Allogeneic mesenchymal stem cells regenerate bone in a critical-sized canine segmental defect. *J Bone Joint Surg Am.* 2003;85A:1927–35.
- Shabbir A, Zisa D, Leiker M, Johnston C, Lin H, Lee T. Muscular dystrophy therapy by non-autologous mesenchymal stem cells: muscle regeneration without immunosuppression and inflammation. *Transplantation.* 2009;87:1275–82.
- Tse WT, Pendleton JD, Beyer WM, Egalka MC, Guinan EC. Suppression of allogeneic T-cell proliferation by human marrow stromal cells: implications in transplantation. *Transplantation.* 2003;75:389–97.
- Tyndall A, Walker UA, Cope A, Dazzi F, De Bari C, Fibbe W, et al. Immunomodulatory properties of mesenchymal stem cells: a review based on an interdisciplinary meeting held at the Kennedy Institute of Rheumatology Division, London, UK, and 31 October 2005. *Arthritis Res Ther.* 2007;9:301.
- Götherström C. Immunomodulation by multipotent mesenchymal stromal cells. *Transplantation.* 2007;84:S35–7.

14. Kretlow JD, Mikos AG. Review: mineralization of synthetic polymer scaffolds for bone tissue engineering. *Tissue Eng.* 2007;13:927–38.
15. Liu CZ, Han ZW, Hourd P, Czernuszka JT. On the process capability of the solid free-form fabrication: a case study of scaffold moulds for tissue engineering. *Proc Inst Mech Eng H.* 2008;222:377–91.
16. Maiti SK, Ninu AR, Sangeetha P, Mathew DD, Tamilmahan P, Kritaniya D, et al. Mesenchymal stem cells-seeded bioceramic construct for bone regeneration in large critical-size bone defect in rabbit. *J Stem Cells Regen Med.* 2016;12:87–99.
17. Shors EC. Coralline bone graft substitutes. *Orthop Clin North Am.* 1999;30:599–613.
18. Maiti SK, Singh GR. Ceramic biomaterials in reconstructive surgery—a review. *Indian J Vet Surg.* 2003;24:1–10.
19. Ravindran NA, Maiti SK, Palakkara S, Kritaniya D, Mahan T, Kumar N. In vitro osteoinduction potential of a novel silica coated hydroxyapatite bioscaffold seeded with rabbit mesenchymal stem cell. *J Stem Cell Res Ther.* 2016. <https://doi.org/10.15406/jsrt.2016.02.00009>.
20. LeGeros RZ. Properties of osteoconductive biomaterials: calcium phosphates. *Clin Orthop Relat Res.* 2002;395:81–98.
21. Maiti SK, Kumar MU, Srivastava L, Ninu AR, Kumar N. Isolation, proliferation and morphological characteristics of bone marrow derived mesenchymal stem cells (BM-MSC) from different animal species. *Trends Biomater Artif Organs.* 2013;27:29–35.
22. Kaveh K, Ibrahim R, Abubakar MZ, Ibrahim TA. Repair of compact bone critical sized defect with bone tissue engineering in rabbits. *J Appl Anim Res.* 2011;39:108–13.
23. Perumal V, Roberts CS. (ii) Factors contributing to non-union of fractures. *Orthop Trauma.* 2007;21:258–61.
24. Zhang X, Qi YY, Zhao TF, Li D, Dai XS, Niu L, et al. Reconstruction of segmental bone defects in the rabbit ulna using periosteum encapsulated mesenchymal stem cells-loaded poly (lactic-co-glycolic acid) scaffolds. *Chin Med J (Engl).* 2012;125:4031–6.
25. Mankani MH, Kuznetsov SA, Fowler B, Kingman A, Robey PG. In vivo bone formation by human bone marrow stromal cells: effect of carrier particle size and shape. *Biotechnol Bioeng.* 2001;72:96–107.
26. Krebsbach PH, Kuznetsov SA, Satomura K, Emmons RV, Rowe DW, Robey PG. Bone formation in vivo: comparison of osteogenesis by transplanted mouse and human marrow stromal fibroblasts. *Transplantation.* 1997;63:1059–69.
27. Kasten P, Vogel J, Luginbühl R, Niemeyer P, Tonak M, Lorenz H, et al. Ectopic bone formation associated with mesenchymal stem cells in a resorbable calcium deficient hydroxyapatite carrier. *Biomaterials.* 2005;26:5879–89.
28. Wang X, Wang Y, Gou W, Lu Q, Peng J, Lu S. Role of mesenchymal stem cells in bone regeneration and fracture repair: a review. *Int Orthop.* 2013;37:2491–8.
29. Kadiyala S, Young RG, Thiede MA, Bruder SP. Culture expanded canine mesenchymal stem cells possess osteochondrogenic potential in vivo and in vitro. *Cell Transplant.* 1997;6:125–34.
30. Eslaminejad MB, Mirzadeh H, Mohamadi Y, Nickmahzar A. Bone differentiation of marrow-derived mesenchymal stem cells using beta-tricalcium phosphate–alginate–gelatin hybrid scaffolds. *J Tissue Eng Regen Med.* 2007;1:417–24.
31. Tanaka T, Hirose M, Kotobuki N, Tadokoro M, Ohgushi H, Fukuchi T, et al. Bone augmentation by bone marrow mesenchymal stem cells cultured in three-dimensional biodegradable polymer scaffolds. *J Biomed Mater Res A.* 2009;91:428–35.
32. Habibovic P, Yuan H, van der Valk CM, Meijer M, van Blitterswijk CA, de Groot K. 3D microenvironment as essential element for osteoinduction by biomaterials. *Biomaterials.* 2005;26:3565–75.
33. Kon E, Muraglia A, Corsi A, Bianco P, Marcacci M, Martin I, et al. Autologous bone marrow stromal cells loaded onto porous hydroxyapatite ceramic accelerate bone repair in critical-size defects of sheep long bones. *J Biomed Mater Res.* 2000;49:328–37.
34. Jiang X, Cui P, Chen W, Zhao D, Luo J, Li G, et al. Study on the directed inducing process of cartilage cells differentiated from human marrow mesenchymal stem cells. *Zhonghua Er Bi Yan Hou Ke Za Zhi.* 2002;37:137–9.
35. Tu J, Wang H, Li H, Dai K, Wang J, Zhang X. The in vivo bone formation by mesenchymal stem cells in zein scaffolds. *Biomaterials.* 2009;30:4369–76.
36. Kaveh K, Ibrahim R, Ibrahim TA, Mohd Zuki AB. Bone marrow seeded bone graft versus bone graft; compact bone critical sized healing pattern in rabbit. *J Anim Vet Adv.* 2010;9:1588–96.
37. Bruder SP, Jaiswal N, Haynesworth SE. Growth kinetics, self-renewal, and the osteogenic potential of purified human mesenchymal stem cells during extensive subcultivation and following cryopreservation. *J Cell Biochem.* 1997;64:278–94.
38. Frank O, Heim M, Jakob M, Barbero A, Schäfer D, Bendik I, et al. Real-time quantitative RT-PCR analysis of human bone marrow stromal cells during osteogenic differentiation in vitro. *J Cell Biochem.* 2002;85:737–46.
39. Gallagher KA, Liu ZJ, Xiao M, Chen H, Goldstein LJ, Buerk DG, et al. Diabetic impairments in NO-mediated endothelial progenitor cell mobilization and homing are reversed by hyperoxia and SDF-1 alpha. *J Clin Invest.* 2007;117:1249–59.
40. Wallace SR, Oken MM, Lunetta KL, Panoskaltsis-Mortari A, Masellis AM. Abnormalities of bone marrow mesenchymal cells in multiple myeloma patients. *Cancer.* 2001;91:1219–30.
41. Li Y, Zhang C, Xiong F, Yu MJ, Peng FL, Shang YC, et al. Comparative study of mesenchymal stem cells from C57BL/10 and mdx mice. *BMC Cell Biol.* 2008;9:24.
42. Niemeyer P, Schönberger TS, Hahn J, Kasten P, Fellenberg J, Siedkamp N, et al. Xenogenic transplantation of human mesenchymal stem cells in a critical size defect of the sheep tibia for bone regeneration. *Tissue Eng Part A.* 2010;16:33–43.
43. Jäger M, Degistirici O, Knipper A, Fischer J, Sager M, Krauspe R. Bone healing and migration of cord blood-derived stem cells into a critical size femoral defect after xenotransplantation. *J Bone Miner Res.* 2007;22:1224–33.
44. Henriksson HB, Svanvik T, Jonsson M, Hagman M, Horn M, Lindahl A, Brisby H. Transplantation of human mesenchymal stem cells into intervertebral discs in a xenogenic porcine model. *Spine (Phila Pa 1976).* 2009;34:141–8.
45. Bartholomew A, Sturgeon C, Siatkas M, Ferrer K, McIntosh K, Patil S, et al. Mesenchymal stem cells suppress lymphocyte proliferation in vitro and prolong skin graft survival in vivo. *Exp Hematol.* 2002;30:42–8.
46. Le Blanc K, Tammik L, Sundberg B, Haynesworth SE, Ringdén O. Mesenchymal stem cells inhibit and stimulate mixed lymphocyte cultures and mitogenic responses independently of the major histocompatibility complex. *Scand J Immunol.* 2003;57:11–20.
47. Wang L, Lu XF, Lu YR, Liu J, Gao K, Zeng YZ, et al. Immunogenicity and immune modulation of osteogenic differentiated mesenchymal stem cells from Banna minipig inbred line. *Transplant Proc.* 2006;38:2267–9.
48. Einhorn TA. The cell and molecular biology of fracture healing. *Clin Orthop Relat Res.* 1998;355:S7–21.
49. Fakhry M, Hamade E, Badran B, Buchet R, Magne D. Molecular mechanisms of mesenchymal stem cell differentiation towards osteoblasts. *World J Stem Cells.* 2013;5:136–48.
50. Qin Y, Guan J, Zhang C. Mesenchymal stem cells: mechanisms and role in bone regeneration. *Postgrad Med J.* 2014;90:643–7.